JOURNAL OF OPTOELECTRONICS AND ADVANCED MATERIALS, Vol. 10, No. 12, December 2008, p. 3274 - 3278

CeF_3: Tb^{3+}/SiO_2 (core/shell) nanostructure：surface coating and photoluminescence

JIANHUA WU, BING YAN*
Department of Chemistry, Tongji University, Shanghai 200092, China

CeF_3: Tb^{3+}/SiO_2 (Core/Shell) with nanostructure were prepared by a complex method based on the surface modification of CeF_3: Tb^{3+} nanoparticles, which crystallized well with a hexagonal structure. The mean grain size of CeF_3: Tb^{3+} and CeF_3: Tb^{3+}/SiO_2 are 10 nm and 14 nm, respectively. Both of them showed green emission corresponded $^5D_4$ –^7F_J transition of Tb^{3+}, and especially the silica film increased the luminescent intensity and lifetimes of CeF_3: Tb^{3+} nanoparticles.

(Received October 22, 2007; accepted November 27, 2008)

Keywords: Surface Coating, Nanocrystalline materials, Nanostructure, Luminescence

1. Introduction

In recent years, growing efforts have been put into the luminescent materials with nanostructure, which present a broad range of potential applications, such as photoluminescent devices, biological fluorescence labeling, low-threshold lasers, optical amplifiers, and so on [1-7]. For example, Ma *et al*. [8] combined successfully the useful functions of super para-magnetism, luminescence, and surface functionality into one material with nano-architecture by sol-gel method. Valérie Buissette and his co-workers synthesized the nanoparticles constituted of a (Y, Ln)VO_4 crystalline core and stabilized by a lanthanide-citrate complex shell [9]. The construction of complex structure was not only a useful method to develop multi-functional materials but also an effective way to improve the luminescent properties. In the fields of traditional fluorescent materials the strategy to grow a suitable inorganic film around each phosphor particles to form the core/shell structures has been applied as an effective path to increase luminescent efficiency and stability. It was pointed out in earlier study that the luminescence efficiency of nanometer materials was usually lower than that of corresponding bulk materials because of nonradiative decay from defects on the surface of the nanocrystals [10, 11]. Recently that strategy also has been successfully applied in nanometer material systems. For instance, nanocomposite thin films where $ZnGa_2O_4$ nanoparticles were dispersed in fluorides, MgF_2 or LaF_3, were prepared by Hirokinaito et al. [12]. They found that enchantment of the PL emission of the composite films was due to the quantum size effect and the surfaces effects.

A bulk crystal of CeF_3 possesses a hexagonal phase structure with a space group of *P*3h*c*1 (*D*3*d* 4) and lattice constants *a*) 0.713 nm, *c*) 0.729 nm, and there are six molecules in the unit cell. The Ce^{3+} ion in the CeF_3 crystal is coordinated by nine F^- and has a C_2 site symmetry. Because of the weaker diffuseness of their electron cloud, and broader energy gap, and low vibrational energies, which lead to the minimization of the quenching of the excited state of the rare-earth ions, lanthanide fluorides are useful luminescent host materials. As a potential scintillator and tunable laser material, CeF_3 is a luminescent material with 100 % activator concentration. Therefore nanometer CeF_3 crystal was often used to study the luminescent properties. Some works about the synthesis of luminescent and optical materials based on CeF_3 nanostructure material were published. S. Eiden-Assmann and G. Maret [13] reported a polyol method to synthesize CeF_3 particles 5 – 10 nm in size. They also claimed that this material had a potential application in novel functional film with tunable magneto-optical properties. Liu *et al*. [14] presented the synthesis of monodispersive CeF_3 nanoparticles with different size from polyisobutene-butanediimede (T154) /cyclohexaner/water microemulsions. However in this case there was little work to grow SiO_2 films around CeF_3 nanoparticles. This paper totally concerned the synthesis and the fluorescent and thermal properties of CeF_3 nanometer crystal coated SiO_2, which form CeF_3: Tb^{3+}/SiO_2 (Core/Shell) nanostructure and result in luminescence enhancement though the surface modification.

2. Experimental

Synthesis. A complex process was adopted to prepare CeF_3: Tb^{3+}/SiO_2 (core/shell) nanostructure based on the preparation of CeF_3:Tb^{3+} nanoparticles by a glycol method [15]. La_2O_3 (99.99 %, Sinopharm Group Chemical

Reagent Co., Ltd. China), Tb_4O_7 (99.99 %, Sinopharm Group Chemical Reagent Co., Ltd.), $Ce(NO_3)_3 \cdot 6H_2O$ (99.99 %, Sinopharm Group Chemical Reagent Co., Ltd. China), NH_4F (99.0 %, analytical reagent, A. R., Sinopharm Group Chemical Reagent Co., Ltd. China), and TEOS($[Si(C_2H_5O)_4]$ 99.0 %, Sinopharm Group Chemical Reagent Co., Ltd. China) were used as starting materials without any further purification. $La(NO_3)_3$ and $Tb(NO_3)_3$ were prepared by dissolving the corresponding oxides in diluted nitric acid, and the water in the solutions was distilled off by heating carefully.

CeF_3: Tb^{3+} nanoparticles. The doping concentration of Tb^{3+} in CeF_3 host was 10 mol %. Stoichiometric amounts of $Ce(NO_3)_3$ and $Tb(NO_3)_3$ (totally 2.0 mmol) were dissolved in 25 mL of DEG at 90 ℃ under stirring to form a clear solution. The solution was then heated in a silicon oil bath under vigorous stirring with a flow of Ar atmosphere, and the temperature of the solution was further increased to 200 ℃. At this temperature, a solution of DEG (25 mL) containing 6 mmol of NH_4F was slowly injected into the above solution, and the mixture was kept at 200 ℃ for 1 h. Then, the obtained suspension was divided into two parts in volume uniformly. The one was cooled to room temperature and diluted with 25mL of ethanol. The solid particles were separated by centrifugation at a speed of 4500 rpm. To remove residual DEG, the solid powders were dispersed in ethanol and centrifuged again. The other one was used to prepare CeF_3: Tb^{3+}/SiO_2 (core/shell) nanostructure

CeF_3: Tb^{3+}/SiO_2 (Core/Shell) nanostructure. The CeF_3: Tb^{3+} / SiO_2 (core/shell) nanostructure was prepared by a further hydrolyzation process of TEOS around the obtained CeF_3: Tb^{3+} nanoparticles. Firstly, 50 mL of anhydrous ethanol and 2.0 mmol TEOS was added to the other one and heated to 120 ℃ for 1 hour with continuous stirring. Then 5 mL NH_4OH was added into the mixture by dropwise under continuous stirring in a silicon oil bath with a flow of Ar. And the suspension was kept at 160 ℃ for 0.5 h. The following procedures were same as those for the synthesis of CeF_3: Tb^{3+} nanoparticles as stated above.

Characterization. X-ray diffraction (XRD) was carried out on a Bruck D8-Advance diffractometer with CuKα radiation (0.15405 nm). The accelerating voltage and emission current were 40 kV and 40 mA, respectively. TEM images were obtained using a JEOL 1230 transmission electron microscope operating at 200 kV. Samples for TEM were prepared by depositing a drop of a colloidal ethanol solution of the powder sample onto a carbon coated copper grid. The excess liquid was wicked away with filter paper, and the grid was dried in air. Chemical analyses are performed by EDX using Philps XL-30 equipments. Fourier transform infrared (FTIR) spectra were measured within the 4000-400 cm^{-1} region on an (Nicolet model 5SXC) infrared spectrophotometer with the KBr pellet technique. The excitation and emission spectra were taken on a RF-5301 spectrophotometer whose excitation and emission slits width were both 3 nm. All the emission and excitation spectra were corrected and the intensities were determined with integrated area. Luminescent lifetimes for hybrid materials were obtained with an Edinburgh Instruments FLS 920 phosphorimeter using a 450 W xenon lamp as excitation source (pulse width, 3 μs).

3. Results and discussion

3.1 Microstructure and Morphology of the Nanocrystals

We investigated the phase structures of the nanoparticles by X-ray powder diffraction. Fig. 1 gives XRD patterns of CeF_3: 10%Tb (a), and CeF_3: 10%Tb/SiO_2 core/shell (b) nanostructure. The reference lines for CeF_3 provided in the JCPDS database (No. 08-0045) are also displayed. Deduced from the XRD data, these two samples are well-crystallized, and both patterns are in good agreement with hexagonal phase structure known from the bulk CeF_3 crystal. This also suggests that the doped Tb^{3+} ions uniformly enter into CeF_3 crystal lattice to form homogeneous solid solution without hybrid phase to be found in XRD peaks. For our CeF_3: 10%Tb/SiO_2 core/shell system, no obvious distinction is observed for the diffraction peaks with respect to those of the CeF_3: 10%Tb core nanoparticles, (as shown in Figure 1), which indicate that SiO_2 does not crystallize well and exists as amorphous substance. Besides, all peaks broaden obviously owing to the small size of the particles. The crystallite sizes can be estimated from the Scherrer equation, $D = 0.941\lambda/\beta\cos\theta$, where D is the average grain size, λ is the X-ray wavelength (0.15405 nm), and θ and β are the diffraction angle and full-width at half-maximum (fwhm) of an observed peak, respectively. The strongest and independent peak (111) at 2θ = 27.8 ° was used to calculate the grain size of the materials.

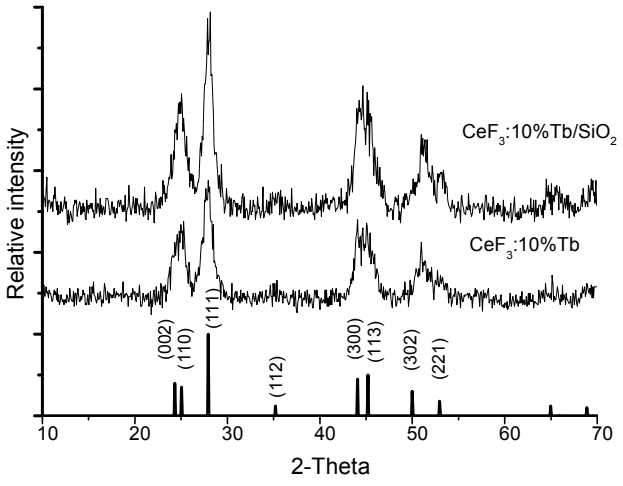

Fig. 1 The XRD patterns of the samples.

3.2 Microstructure and Morphology

TEM were performed to observe the morphology of the obtained samples. And the micrographs are shown in Fig. 2. Fig. 2a gives the image of CeF_3: 10%Tb particles magnified 500,000 times. From the picture the size of CeF_3: 10%Tb particles is about 7-10 nm, and the shape is fairly regular, also agglomeration between the particles is slight. The image of CeF_3: 10%Tb/SiO_2 material was shown in Fig.2b. The results demonstrate that there is a little difference between the two samples: the particle size of CeF_3: 10%Tb/SiO_2 is bigger than that of CeF_3: 10%Tb, which does not take in good agreement with of XRD results (see in table 1). As we known that the size result caculated from Scherrer equation only gives the size of the CeF_3 single crystal, which is same in two samples. Therefore the calculated size of the particles of CeF_3: 10%Tb/SiO_2 is similar with that of CeF_3. But the real size of CeF_3: 10%Tb/SiO_2 particles, which contains CeF_3 crystallite and amorphous silica shell, is the sum of the size of CeF_3 and the double thickness of silica film. Based on the size analysis from Fig. 2b, the thickness of silica film is about 2 nm. The lattice fringes of crystalline CeF_3: 10%Tb can be seen more clearly than that of CeF_3: 10%Tb/SiO_2. The reason that more interaction between the amorphous silica films lead to the agglomeration of particles is available.

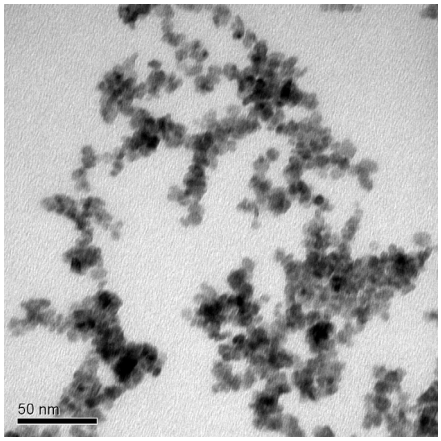

a

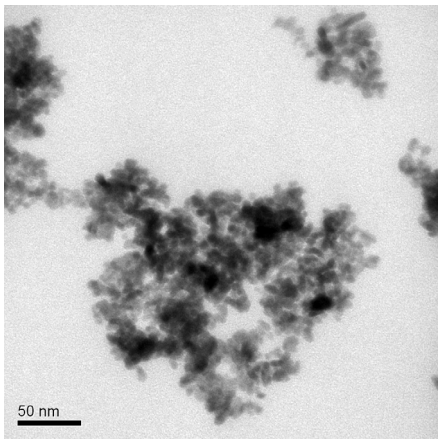

b

Fig. 2 TEM micron morphologies of samples (A): CeF_3: Tb^{3+} and (B): CeF_3: Tb^{3+}/SiO_2.

Table 1. the size of samples from XRD and TEM, respectively.

Size (nm)	CeF_3: 10%Tb nanoparticles	CeF_3: 10%Tb/SiO_2 nanostructure
XRD	8.5	8.0
TEM	10.0	14.0

It is well know that on the alkali conditions TEOS is easy to hydrolysis, so the formation of silica film include the hydrolysis process of TEOS and the polycondensation reaction of the hydroxyl derivatives to form Si-O network. The detailed scheme of the formation of core/shell nanostructure is shown in Fig. 3. To obtain information about the chemical composition of nanoparticles EDX measurements were performed. The EDX spectrum (Fig. 4) suggests that Si and O are only detected on the CeF_3: 10%Tb/SiO_2 sample, which conform that TEOS hydrolyzed successfully.

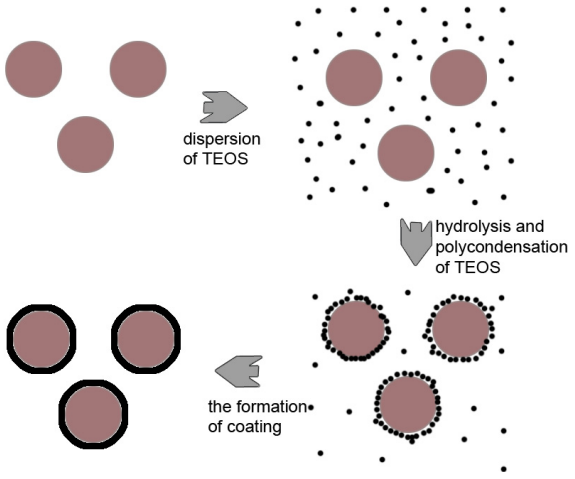

Fig. 3 The scheme of the formation process of core/shell nanostructure.

Fig. 5(a, b) shows the FT-IR spectra of CeF_3: 10%Tb (a), and CeF_3: 10%Tb/SiO_2, respectively. It should be noted that some main absorption peaks observed at approximately 1591, 1508, 1385 cm^{-1}, can be attributed to the remanent organic solvent. There is distinct difference between the two spectra. And a strong and broad absorption band in CeF_3: 10%Tb/SiO_2 are observed at approximately 800 cm^{-1}, which is attributed to the antisymmetric stretching vibration of Si–O bonding of silica.

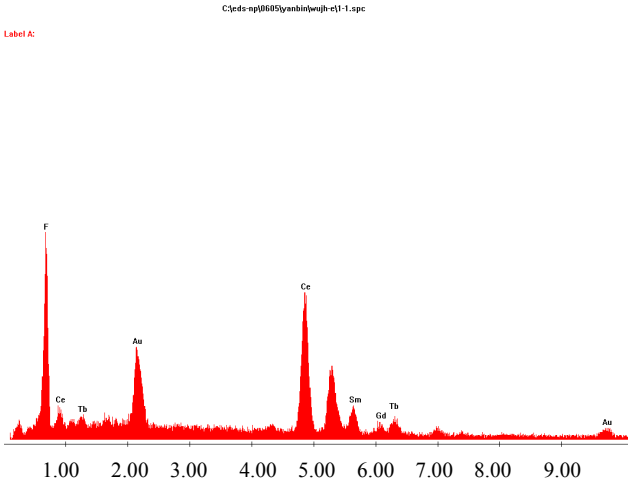

a

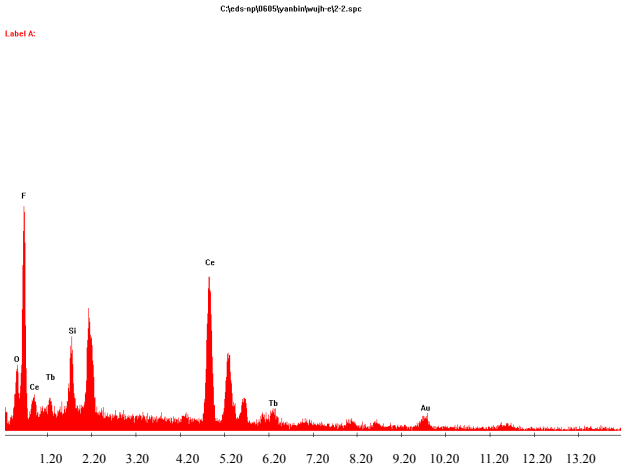

b

Fig. 4 Energy dispersive X-ray spectra of obtained samples (A): CeF_3: Tb^{3+} and (B): CeF_3: Tb^{3+}/SiO_2.

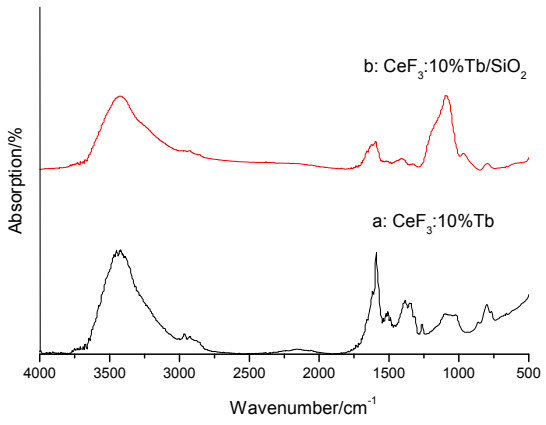

Fig. 5 The FT-IR spectra of CeF_3: 10%Tb (a), and CeF_3: 10%Tb/SiO_2.

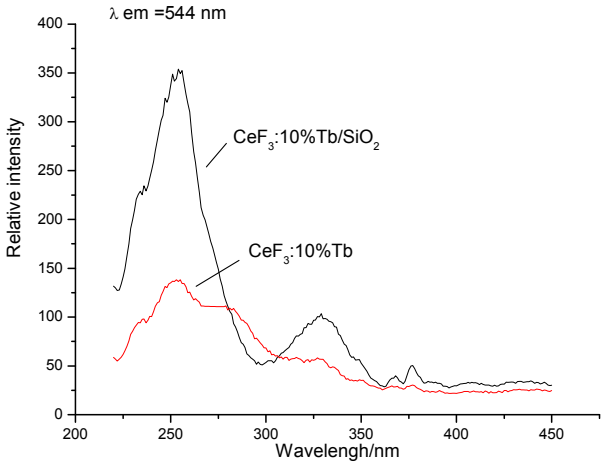

a

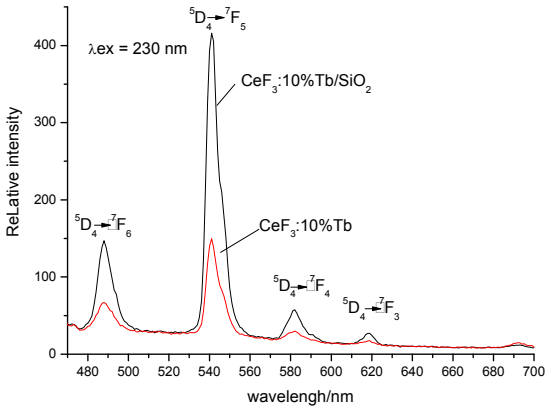

b

Fig. 6 The Excitation (A) and emission (B) spectra of CeF_3: 10%Tb and CeF_3: 10%Tb/SiO_2.

3.3 Luminescent properties

The luminescent spectra of trivalent lanthanide ions in phosphors are mainly from two types of electronic transitions: 4 *f* – 4 *f* transition and 5 *d* – 4 *f* transition. The former generally shows sharp emission line, while the latter have a broad band character. Fig. 6(A) is the room temperature excitation spectral of samples CeF_3: 10%Tb (a) and CeF_3: 10%Tb/SiO_2 (b). The excitation spectra were obtained by monitoring the $^5D_4$ – $^7F_5$ transition of Tb^{3+} ions (543 nm). It can be clearly shown that the excitation spectra consist of two parts, one broadband in the 240-300 nm region resulted from the well-known $^2F_{5/2}$ – 5d (or 4f – 5d) transition of Ce^{3+} and several sharp peaks in 320 – 500 nm region related to the f-f transitions of Tb^{3+} ions. Fig. 6 (B) shows the emission spectra of the obtained sample which were measured under 310 nm excitation at the room temperature. The sharp emission peaks originates from the 4f – 4f transition of Tb^{3+} ions: $^5D_4$ – $^7F_6$ (488 nm) , $^5D_4$ –

$^7F_5$ (541 nm) $^5D_4$ – $^7F_4$ (583 nm) and very weak $^5D_4$ – $^7F_4$ (433 nm). $^5D_4$ – $^7F_5$ (413 nm). In addition, the spectra of two samples both suggest that silica film can increase the luminescent intensities, which may be caused by the coated silica film. Furtherly, the luminescent lifetimes for CeF_3: 10%Tb (a) and CeF_3: 10%Tb/SiO_2 are 0.74 ms and 0.97 ms, suggest the surface coating can effectively decrease the nonradiative transition. Although the quantum efficiency of Tb system is too complicated to be calculated from the lifetime data, we still predict that the quantum efficiency for CeF_3: 10%Tb/SiO_2 may be higher than CeF_3: 10%Tb because it possess longer lifetime [16-18].

4. Conclusion

In summary, CeF_3: Tb^{3+}/SiO_2 (Core/Shell) nanostructure luminescent materials were successfully prepared by a complex method based on preparation of CeF_3: Tb^{3+} nanoparticles. XRD measurement indicated that the obtained CeF_3: Tb^{3+}, and CeF_3: Tb^{3+}/SiO_2 (Core/Shell) nanometer materials crystallized well. And the amorphous silica shell had not influence on the lattice parameters of CeF_3: Tb^{3+}. FI-IR spectra and EDX results suggest the existence of SiO_2 on the surface of the particles. The TEM images illustrated that the mean grain size of CeF_3: Tb^{3+} and CeF_3: Tb^{3+}/SiO_2 are 10 nm and 14 nm, respectively. Under 254nm UV lamp CeF_3: $Tb^{3+}$and CeF_3: Tb^{3+}/SiO_2 both showed green emission, and fluorescent experiments revealed that the both nanometer materials showed the characteristic emission of Tb^{3+} $^5D_4$ $-^7F_J$ (J = 6, 5, 4, 3) transition, with the strongest one at 542 nm. The luminescent properties also revealed that the silica film increased the luminescent intensity and lifetimes of CeF_3: Tb^{3+} nanoparticles.

Acknowledgements

The work was supported by the Science Fund of Shanghai University for Excellent Youth Scientists and National Natural Science Foundation of China (20671072).

References

[1] J. S. Steckel, J. P. Zimmer, S. Coe-Sullivan, Angew. Chem. Int. Ed. **43,** 2154 (2004).
[2] Z. W. Quan, Z. L. Wang, P. P. Yang, Inorg. Chem. ASAP (2007).
[3] V. Salgueiriño-Maceira, M. A. Correa-Duarte, M. Spasova, Adv. Funct. Mater. 16 (2006) 509.
[4] A. Mayer, S. Neuenhofer, Angew. Chem. Int. Ed. **33**, 1044 (1994).
[5] J. W. Gerald, A. Hebbink, J. Huskens, Chem. Mater. **15**, 4604 (2003).
[6] W. Tan, K. Wang, X. He, Med. Res. Rev. **24**, 621 (2004).
[7] V. Buissette, M. Moreau, T. Gacoin, Adv. Funct. Mater. **16**, 351 (2006).
[8] D. Ma, J. Guan, F. Normadin, Chem. Mater. **18**, 1920 (2006).
[9] V. Buissette, A. Huignarda, K. Lahlila, Proc. of SPIE **5222**, 141 (2003).
[10] W. Bu, Z. Hua, H. Chen, J. Shi, J. Phys. Chem. B **109**, 14461 (2005).
[11] Q. Li, L. Gao, D. Yan, Chem. Mater. **11**, 533 (1999).
[12] H. Naito, S. Fujihara, T. Kimura, J. Sol-Gel Sci. Technol. **26**, 997 (2003).
[13] S. Eiden-Assmann, G. Maret, Mater. Res. Bull. **39**, 21 (2004).
[14] S. Q. Qiu, J. X. Dong, G. X. Chen, Powder Technol. **113**, 9 (2000).
[15] Z. L. Wang, Z. W. Quan, P. Y. Jia, Chem. Mater. **18**, 2030 (2006).
[16] M. H. V. Werts, R. T. F. Jukes, J. W. Verhoeven, Phys. Chem. Chem. Phys. **4**, 1542 (2002).
[17] O. L. Malta, M. A. Couto dos Santos, L. C. Thompson, N. K. Ito, J. Lumin. **69**, 77 (1996).
[18] O. L. Malta, H. F.Brito, J. F. S. Menezes, F. R. Gonc¸alves e Silva, Alves, F. S. Farias, A. V. M. Andrade, J. Lumin. 75, 255 (1997).

*Corresponding author: byan@tongji.edu.cn